

Optical polarization characteristics for AlGaN-based light-emitting diodes with AlGaN multilayer structure as well layer

Lu Xue(薛露), Yi Li(李毅), Mei Ge(葛梅), Mei-Yu Wang(王美玉), and You-Hua Zhu(朱友华)
Citation: Chin. Phys. B, 2021, 30 (**4**): 047802. DOI: 10.1088/1674-1056/abcf3f
Journal homepage: http://cpb.iphy.ac.cn; http://iopscience.iop.org/cpb

What follows is a list of articles you may be interested in

Effect of Sb composition on the band alignment of InAs/GaAsSb quantum dots

Guangze Lu(陆光泽), Zunren Lv(吕尊仁), Zhongkai Zhang(张中恺), Xiaoguang Yang(杨晓光), and Tao Yang(杨涛)
Chin. Phys. B, 2021, 30 (**1**): 017802. DOI: 10.1088/1674-1056/abb309

Photoluminescence of green InGaN/GaN MQWs grown on pre-wells

Shou-Qiang Lai(赖寿强), Qing-Xuan Li(李青璇), Hao Long(龙浩), Jin-Zhao Wu(吴瑾照), Lei-Ying Ying(应磊莹), Zhi-Wei Zheng(郑志威), Zhi-Ren Qiu(丘志仁), and Bao-Ping Zhang(张保平)
Chin. Phys. B, 2020, 29 (**12**): 127802. DOI: 10.1088/1674-1056/abb65b

Photoluminescence properties of blue and green multiple InGaN/GaN quantum wells

Chang-Fu Li(李长富), Kai-Ju Shi(时凯居), Ming-Sheng Xu(徐明升), Xian-Gang Xu(徐现刚), Zi-Wu Ji(冀子武)
Chin. Phys. B, 2019, 28 (**10**): 107803. DOI: 10.1088/1674-1056/ab4046

Improvement of TE-polarized emission in type-Ⅱ InAlN-AlGaN/AlGaN quantum well

Yi Li(李毅), Youhua Zhu(朱友华), Meiyu Wang(王美玉), Honghai Deng(邓洪海), Haihong Yin(尹海宏)
Chin. Phys. B, 2019, 28 (**9**): 097801. DOI: 10.1088/1674-1056/ab343a

High-efficiency InGaN/AlInGaN multiple quantum wells with lattice-matched AlInGaN superlattices barrier

Feng Xu(徐峰), Peng Chen(陈鹏), Fu-Long Jiang(蒋府龙), Ya-Yun Liu(刘亚云), Zi-Li Xie(谢自立), Xiang-Qian Xiu(修向前), Xue-Mei Hua(华雪梅), Yi Shi(施毅), Rong Zhang(张荣), You-Liao Zheng(郑有炓)
Chin. Phys. B, 2017, 26 (**1**): 017803. DOI: 10.1088/1674-1056/26/1/017803

Optical polarization characteristics for AlGaN-based light-emitting diodes with AlGaN multilayer structure as well layer*

Lu Xue(薛露), Yi Li(李毅)†, Mei Ge(葛梅), Mei-Yu Wang(王美玉), and You-Hua Zhu(朱友华)

School of Information Science and Technology & Tongke School of Microelectronics, Nantong University, Nantong 226019, *China*

(Received 20 August 2020; revised manuscript received 24 November 2020; accepted manuscript online 1 December 2020)

The optical properties of AlGaN-based quantum well (QW) structure with two coupled thin well layers are investigated by the six-by-six $\boldsymbol{K}$–$\boldsymbol{P}$ method. Compared with the conventional structure, the new structure, especially the one with lower Al-content in the barrier layer, can enhance the TE-/TM-polarized total spontaneous emission rate due to the strong quantum confinement and wide recombination region. For the conventional QW structure, the reduction of well thickness can lead the degree of polarization (DOP) to decrease and the internal quantum efficiency (IQE) to increase. By using the coupled thin well layers, the DOP for the structure with high Al-content in the barrier layer can be improved, while the DOP will further decrease with low Al-content in the barrier layer. It can be attributed to the band adjustment induced by the combination of barrier height and well layer coupling. The IQE can also be further enhanced to 14.8%–20.5% for various Al-content of barrier layer at $J = 100$ A/cm^2. In addition, the efficiency droop effect can be expected to be suppressed compared with the conventional structure.

Keywords: AlGaN-based quantum well, $\boldsymbol{K}$–$\boldsymbol{P}$ method, internal quantum efficiency, degree of polarization

PACS: 78.66.Fd, 78.67.De, 78.67.–n, 78.67.Pt **DOI:** 10.1088/1674-1056/abcf3f

1. Introduction

AlGaN-based deep ultraviolet (DUV) light-emitting diodes (LEDs) have attracted much attention due to their broad application prospects in water purification, sterilization, skin therapy, *etc*.[1–4] To date, the external quantum efficiency (EQE) of AlGaN-based DUV LED bare die with a p-GaN contact layer is generally less than 7% at 250 nm–280 nm.[4] Compared with blue LED, AlGaN-based DUV LED has high acceptor ionization energy, strong absorption in the p-GaN contact layer, and unique polarization characteristics, which makes it have lower EQE.[5,6] In order to solve these problems, many methods have been used to improve the luminous efficiency of AlGaN-based DUV LED. For example, by employing several features, such as the AlGaN:Mg contact layer and Rh mirror electrode, Takano *et al*. reported that a maximum EQE of more than 20% can be obtained at 275 nm.[7] Wang *et al*. proposed an ultrathin GaN/AlN multiple quantum wells (MQWs) structure with electron-beam pumping.[6] The output power of MQWs reached ~ 2.2 W at 260 nm due to the reduction of quantum-confined Stark effect (QCSE) and the improvement of material quality and carrier injection. Zhang *et al*. proposed a DUV LED structure with air cavity extractor, which can significantly improve the extraction efficiency of TM/TE polarized light.[8] In addition, in order to improve the luminous efficiency of LED, other structure designs have also been reported in the literature, such as the multi-quantum barrier electron blocking layer structure,[9] the type-II QW structure,[5,10] AlN-delta-GaN QW structure,[11] step-like QW structure,[12,13] and Al composition-graded p-AlGaN cladding layer structure.[14]

In our previous work, we reported the effects of Al-content in the barrier layer on the optical properties of $Al_{0.35}Ga_{0.65}N/Al_xGa_{1-x}N$ QW structure.[15] By increasing the Al-content of barrier layer, the degree of polarization (DOP) can be greatly improved. However, the spontaneous emission rate for TM mode and TE mode decrease with the increase of Al composition in the barrier layer due to the larger polarization-induced electric field. Although the effect of the internal electric field on the electron–hole overlap can decrease by reducing the thickness of the well layer, the further improvement of the spontaneous emission rate will be limited due to the decrease of the electron-hole radiation recombination region.

In the present paper, we propose an $Al_yGa_{1-y}N$-$Al_xGa_{1-x}N$-$Al_yGa_{1-y}N/Al_xGa_{1-x}N$ QW structure. Here, the multilayer structure as the new well layer consists of two thin $Al_yGa_{1-y}N$ well layers separated by a thin $Al_xGa_{1-x}N$ isolation layer. Replacing a conventional well layer with two coupled well layers can not only suppress the QCSE, but also effectively increase the electron–hole recombination region. The numerical results show that the TE/TM polarized emission and internal quantum efficiency (IQE) can be significantly improved by using two coupled QW structures, while the DOP can be similar to that of conventional quantum well structure.

*Project supported by the National Natural Science Foundation of China (Grant No. 61874168), the Jiangsu Province I-U-R Cooperation Project, China (Grant No. BY2019114), and the Nantong Science and Technology Project, China (Grant No. JC2019006).

†Corresponding author. E-mail: liyi2016@ntu.edu.cn

© 2021 Chinese Physical Society and IOP Publishing Ltd

2. Theory

The optical properties of AlGaN-based LEDs were investigated by solving the Schrödinger–Posisson equations self-consistently. In order to calculate the valence structure, the block-diagonalized 6×6 $\boldsymbol{K}$–$\boldsymbol{P}$ Hamiltonian was adopted, which can be expressed as[16]

$$H^{v}=\begin{pmatrix} H^{\mathrm{U}} & 0 \\ 0 & H^{\mathrm{L}} \end{pmatrix}. \tag{1}$$

Here, H^{U} and H^{L} are the 3×3 upper and lower Hamiltonians. The conduction band structure was solved by the single band effective mass Hamiltonian given in Refs. [5,17]. In calculations, the finite difference method with a 1-Å interval was employed to solve the Schrödinger–Posisson equations.[17] The quasi-Fermi energy level difference between electron and hole is used as an input parameter.[18] The model used here is based on the model reported in Ref. [18], which can accurately calculate the Hartree potential, energy bands, and wave functions. The material parameters of GaN and AlN have been introduced in Refs. [5,15,19]. The corresponding material parameters of ternary alloy AlGaN can be obtained by the linear interpolation method except the band-gap, spontaneous polarization, and crystal-field splitting energy.

After obtaining the conduction band structure, the valence band structure, and the corresponding wave function, the spontaneous emission rate (r^{spon}) was solved by the following formula:[19]

$$r^{\mathrm{spon}}(\hbar\omega)=\left(\frac{8\pi n_r^2\hbar^2\omega^2}{h^3c^2}\right)C_0\frac{2}{L_z}\sum_{\sigma}\sum_{n,m}\int_0^{\infty}\frac{k_{\mathrm{t}}\mathrm{d}k_{\mathrm{t}}}{2\pi}M^{\sigma}_{nm}(k_{\mathrm{t}})f_c^n \times(1-f_v^{\sigma m})\frac{\Gamma/\pi}{[E^{cv}_{\sigma,nm}(k_{\mathrm{t}})-\hbar\omega]^2+\Gamma^2},$$

with

$$C_0=\frac{\pi e^2}{n_r c\varepsilon_0 m_o^2\omega}, \tag{2}$$

where L_z is the active layer thickness, k_t is the in-plane wave vector, $M^{\sigma}_{nm}(k_{\mathrm{t}})$ is the optical momentum matrix element, f_c^n and $f_v^{\sigma m}$ are the Fermi–Dirac distribution functions, Γ is the line-width, $E^{cv}_{\sigma,nm}(k_{\mathrm{t}})$ is the transition energy between the n-th conduction sub-band and the m-th valence sub-band.

3. Results and discussion

In this work, the AlGaN-based LED with an AlGaN multilayer structure as the well layer is considered, including an n-type $Al_{0.55}Ga_{0.45}N$ layer, a single QW (SQW) layer, and a p-type $Al_{0.5}Ga_{0.5}N$ layer, which are shown in Fig. 1. The SQW consists of an 8-nm-$Al_xGa_{1-x}N$ barrier layer and two 1-nm-$Al_{0.35}Ga_{0.65}N$ well layers separated by 2-nm-$Al_xGa_{1-x}N$ isolation layer. The barrier layer and the isolation layer have the same Al component, and the Al component x values are set to be 0.5 and 0.55, which are called samples A and A_1 respectively. For comparison, the conventional QW structures with 1 nm (sample B, B_1) and 2.5 nm (sample C, C_1) $Al_{0.35}Ga_{0.65}N$ well layer are also studied. The value of x in Al composition of the $Al_xGa_{1-x}N$ barrier layer of samples B and C are both set to be 0.5, while that of samples B_1 and C_1 are both set to be 0.55. The electron concentration and hole concentration of n-type and p-type layers are set to be 1.7×10^{18} cm^{-3} and 2.74×10^{17} cm^{-3}, respectively.

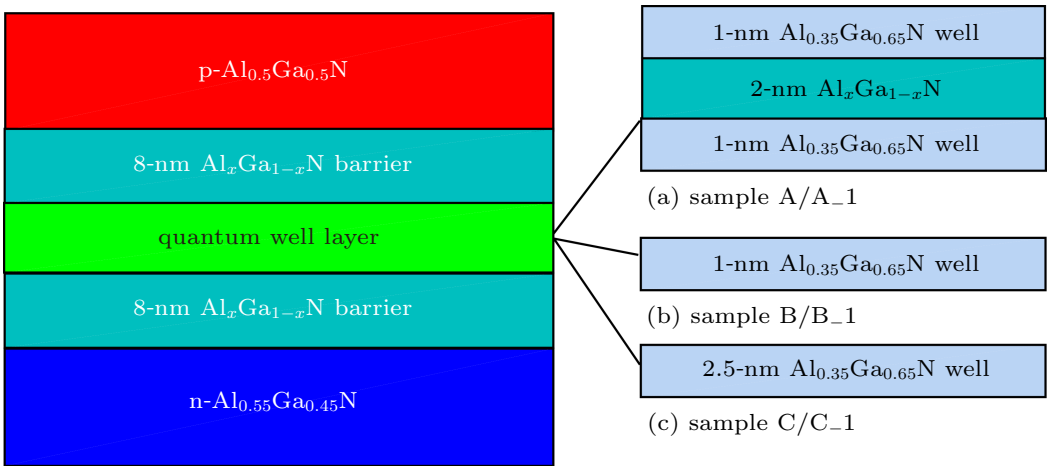


Fig. 1. Schematic structure of samples A (A_1), B (B_1), and C (C_1).

Figure 2 shows the TE-polarized and TM-polarized spontaneous emission spectra of the samples A (A_1), B (B_1), and C (C_1) at the injection current density of 100 A/cm^2. The injection current density (J) can be expressed as $J=q(R_{\mathrm{cr}}+R_{\mathrm{nonr}}+R_{\mathrm{Aug}})$. The R_{cr} is the average value of two TE-polarized R_{sp} values and one TM-polarized R_{sp} value. Here, the R_{sp} can be obtained from $R_{\mathrm{sp}}=L_z\int_0^{\infty}r^{\mathrm{spon}}(\hbar\omega)\mathrm{d}\hbar\omega$. The R_{nonr} and R_{Aug} are the Shockley–Read–Hall (SRH) recombination rate and the Auger recombination rate per unit area, respectively. The SRH recombination lifetime and the Auger

coefficient are set to be 10 ns and 5×10^{-30} cm^6/s.[20] From the figure, it can be clearly seen that the spontaneous emission rate of both TE and TM polarizations decreases with the Al composition in the barrier layer increasing. It has been reported in our previous study that the increase of Al composition in the barrier layer will lead the internal electric field to increase, resulting in the decrease of radiation recombination rate.[15] For the traditional quantum well structure, with the decrease of the thickness of the well layer, the spontaneous emission rate increases obviously due to the quantum confinement effect, and the peak wavelength also shifts towards the short wavelength. Comparing with samples B and B_1, the TE/TM mode peak intensity for the corresponding novel structures (samples A and A_1) is lower, due to the larger active layer thickness L_z. However, the novel structure shows a larger total spontaneous emission rate, which will be described below.

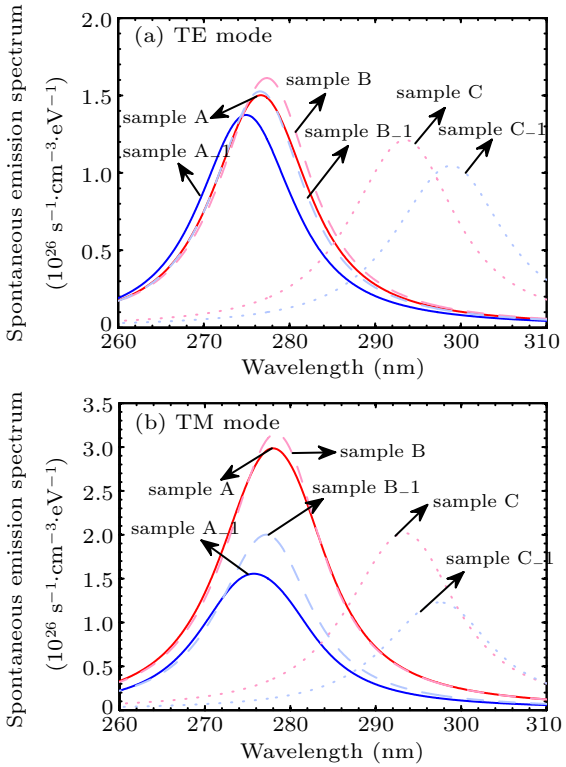


Fig. 2. (a) TE-polarized and (b) TM-polarized spontaneous emission spectra of the samples A (A_1), B (B_1), and C (C_1) at $J = 100$ A/cm^2.

Figure 3 shows TE-polarized and TM-polarized total spontaneous emission rate (R_{sp}) as a function of current density. As mentioned in our previous investigation,[15] the R_{sp} for TE mode and TM mode can be improved by reducing the Al content of the barrier layer, which is caused by the decrease of internal electric field. When the injection current density is greater than about 35 A/cm^2, the TE-polarized and TM-polarized R_{sp} of novel structure (sample A) are larger than those of the traditional quantum well structure (sample B). With the increase of Al-content of barrier layer, the TE-polarized R_{sp} of the new structure (sample A_1) is obviously larger than that of the conventional structure (sample B_1) at $J > 56$ A/cm^2, while the TM-polarized R_{sp} of sample A_1 is slightly larger at $J > 85$ A/cm^2. For example, at $J = 100$ A/cm^2, the TE-polarized and TM-polarized R_{sp} of sample A are increased by 12.7% (35.6%) and 17.7% (67.7%), compared with those of sample B (sample C), while those of sample A_1 are increased by 9.6% (44.3%) and 1.8% (51.1%) respectively compared with those of sample B_1 (sample C_1). The higher R_{sp} for the novel structure can be attributed to the strong quantum confinement and the wide recombination region.

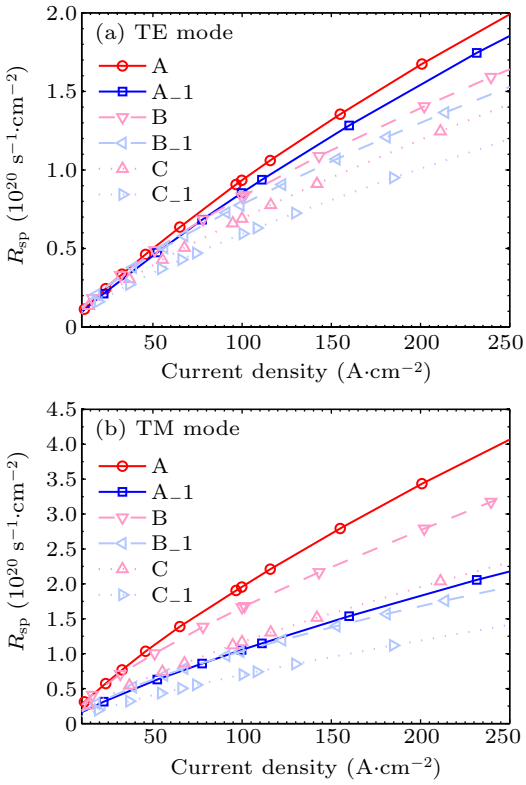


Fig. 3. The total spontaneous emission rate (R_{sp}) for TE polarization (a) and TM polarization (b) as a function of current density.

Figure 4 shows the peak wavelength of TE-mode and TM-mode as a function of current density. It can be seen from the figure that the peak wavelength of TM-mode is greater than that of TE-mode, except samples C and C_1. At the injection current density of 100 A/cm^2, the difference in peak wavelength between the TM mode and the TE mode increases from -0.14 nm (-1.3 nm) of sample C (C_1) to 1.36 nm (0.79 nm) of sample A (A_1). As shown in Figs. 5(b) and 5(c), the difference between c1–v2 and c1–v1 transitions at Γ point is obviously increased by reducing the well layer thickness of conventional QW structure. In this paper, the c1 and c2 denote the two lowest conduction subbands and the v1–v6 represent the top six valence subbands, obtained by using the upper Hamiltonian. For the novel structure, the transition energy levels

extend to a wide energy range due to the coupling between well layers as shown in Fig. 5(a). In addition, the dominant polarization properties of the transition energy levels are different, which can be inferred from the peak intensities of TE mode and TM mode in Figs. 5(d)–5(f). Thus, the difference in peak wavelength between the two polarization modes can be increased by the strong quantum confinement and the coupling between the well layers. It should be noted that the peak wavelength of TE mode for samples C and C_1 are longer than the peak wavelength of TM mode. Although the dominant polarization of c1–v1 and c1–v2 transitions of sample C (or C_1) are TM polarization and TE polarization respectively as inferred from Fig. 5(f), the differences in peak intensity between TM mode and TE mode for both c1–v1 and c1–v2 transitions are much smaller than counterparts of sample B. In addition, for c1–v1 transition, the TE-mode peak wavelength is longer than TM-mode peak wavelength (not given here). These factors lead to longer peak wavelength of TE mode. It is also found that the peak wavelength of TM mode of sample A (A_1) is longer than that of sample B (B_1) at low injection current density, while that of TE mode is shorter. It can be attributed to the coupling between the well layers, so that the energy level in the quantum well is split into a lower level and a higher level as shown in Figs. 5(a) and 5(b). Moreover, it can be inferred from Fig. 5(d) that the c1–v1 transition and the c2–v1 transition have a TM-dominated polarization characteristic, while c1–v5 and c2–v2 have a TE-dominated polarization characteristic. Thus, the peak wavelength of TM mode of novel structure can be longer at the low injection current density. At high current density, the peak wavelengths of TM and TE modes of sample A (A_1) are both shorter than those of sample B (B_1) due to the influence of the higher transition energy levels, such as c2–v1 and c2–v2 transitions.

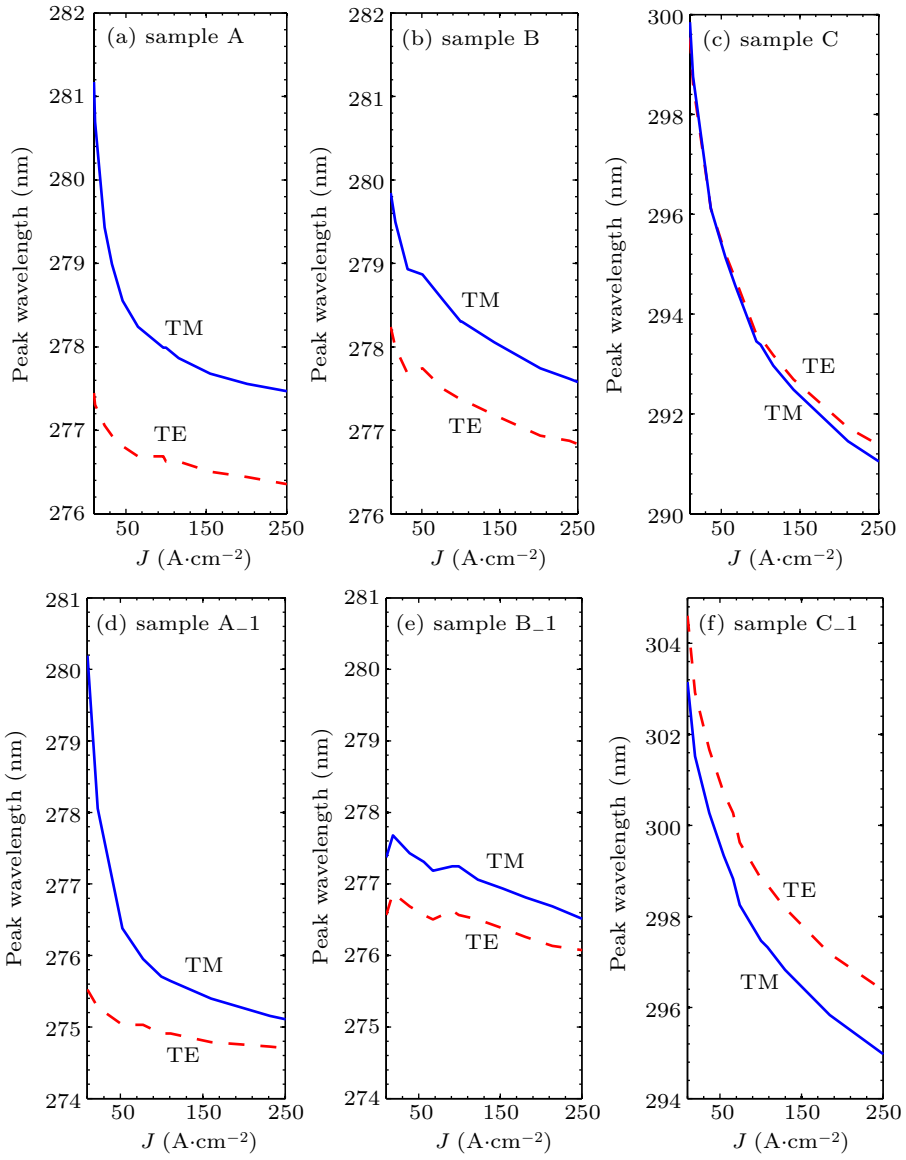


Fig. 4. Plots of peak wavelength of TE mode and TM mode *versus* current density.

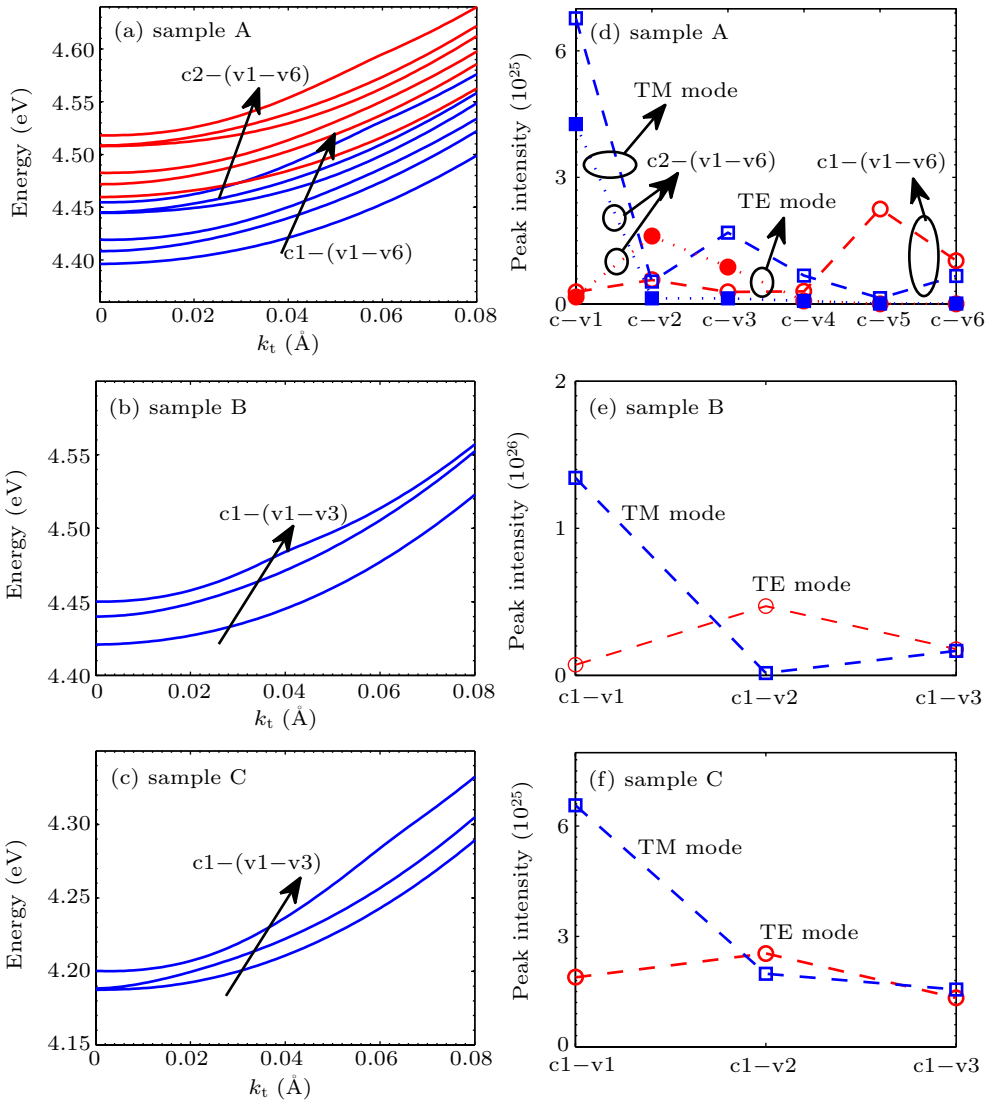


Fig. 5. Plots of (a)–(c) transition energy and (d)–(f) peak intensity for the transitions between the conduction subbands (c1–c2 or c1) and valence subbands (v1–v6 or v1–v3) at $J = 100$ A/cm^2. These valence subbands are obtained by using upper Hamiltonian.

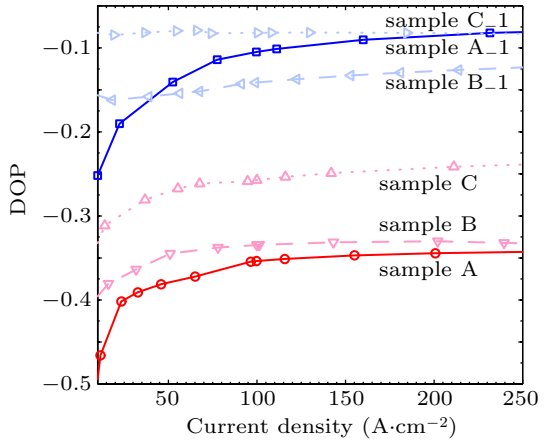


Fig. 6. DOP values *versus* current density for samples A (A_1), B (B_1), and C (C_1).

Figure 6 shows the DOPs as a function of current density for samples A (A_1), B (B_1), and C (C_1). The DOP can be calculated from $\rho = (I_{TE} - I_{TM})/(I_{TE} + I_{TM})$, where I_{TE} and I_{TM} are the TE-polarized and TM-polarized R_{sp}, respectively. On the whole, the QW structure with high Al-content in the barrier layer has a larger DOP value as reported in Ref. [15]. For the conventional QW structure, the DOP decreases with the well layer thickness decreasing from 2.5 nm to 1 nm. Comparing with sample C (C_1), the DOP of sample B (B_1) is reduced by 0.06–0.09 (0.08–0.04) in the investigated injection current density range. From Figs. 5(e) and 5(f), it can be seen that the mixing of valence subbands seems to weaken with the decrease of well thickness, so that the c1–v1 transition of sample B is almost of TM polarization, while the c1–v2 transition is almost of TE polarization. Meanwhile, the difference in transition energy between c1–v1 and c1–v2 becomes larger. As a result, the DOP for the conventional QW structure can decrease by reducing the well thickness. Note that the DOP of sample C is basically consistent with the reported experimental result in Ref. [21] at $J = 100$ A/cm^2. For the novel structure, the DOP of sample A further decreases compared

with those of samples B and C, while the DOP of sample A_1 increases to a value close to the DOP of sample C_1 as the current density increases. From Fig. 5(d) it can follow that the peak intensity of TM mode for the c1–v1 transition and the c2–v1 transition are much larger than the peak intensities of TE mode for all transitions. However, this situation does not occur for sample A_1 with high Al-content in the barrier layer as shown in Fig. 7(a). The peak intensity of TE mode of c1–v4 transition for sample A_1 can be compared with that of TM mode of c1–v1 transition and c2–v1 transition, which is similar to that of c1–v1 transition and c1-v3 transition for sample C_1. Thus, the DOP of sample A can further decrease, while the DOP of sample A_1 is close to that of sample C_1 at the larger current density.

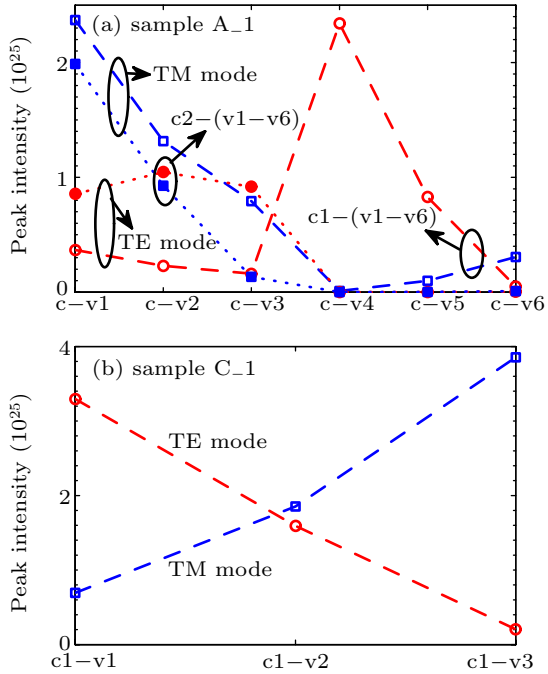


Fig. 7. Peak intensities of TE mode and TM mode for transitions between the conduction subbands (c1–c2 or c1) and valence subbands (v1–v6 or v1–v3) at $J = 100$ A/cm^2 for (a) sample A_1 and (b) sample C_1.

Finally, the internal quantum efficiency for each of samples A (A_1), B (B_1), and C (C_1) as a function of current density is investigated, and the results are shown in Fig. 8. The IQE is defined as $\eta = R_{\rm cr}/(R_{\rm cr}+R_{\rm nonr}+R_{\rm Aug})$.[19] At an injection current density of 100 A/cm^2, it can be observed that the IQE is enhanced from 13.6% (10.1%) of sample C (C_1) to 20.5% (14.8%) of sample A (A_1). It should be noted that the calculated IQE is low, which can be attributed to two factors. One is due to the large Auger coefficient and small SRH recombination lifetime employed in the calculation. According to the reports in the literature,[22,23] the Auger coefficient can be increased from $\sim 10^{-31}$ cm^6/s to $\sim 10^{-30}$ cm^6/s due to the defect-assisted Auger recombination, which will lead the IQE to significantly decrease. The other is that the average value $R_{\rm cr}$ of AlGaN-based LED is lower due to its polarization characteristics than that of visible light GaN-based LED. In addition, it is also seen that the efficiency droop effect can be obviously suppressed by using the novel QW structure. For example, the IQE of sample A (A_1) from $J = 10$ A/cm^2 to $J = 250$ A/cm^2 is reduced by 30.6% (33.3%), while that of samples B (B_1) and C (C_1) are reduced by 48.1% (52.2%) and 48.5% (49.87%), respectively. Comparing with the traditional structure, the performance improvement of the new structure is attributed not only to the enhancement of spontaneous emission rate, but also to the decrease of Auger recombination rate due to the wide recombination region.

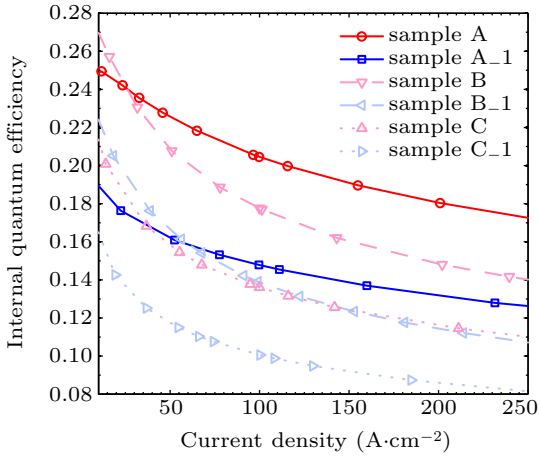


Fig. 8. Plots of internal quantum efficiency of AlGaN-based QW structure *versus* current density for various samples.

4. Conclusions

In this work, the optical properties of AlGaN-based QW structure with two coupled thin well layers are investigated by using the effective mass theory. As the current density is greater than a certain value, the TE- and TM-polarized $R_{\rm sp}$ of sample A (A_1) are larger than those of samples B (B_1) and C (C_1) due to the strong quantum confinement and the wide recombination region. At $J = 100$ A/cm^2, the difference in peak wavelength between TM mode and TE mode increases from -0.14 nm (-1.3 nm) of sample C (C_1) to 1.36 nm (0.79 nm) of sample A (A_1), while the peak wavelength of sample A (A_1) is shorter than the peak wavelengths of samples B (B_1) and C (C_1). For the conventional QW structure, the DOP of sample B (B_1) is reduced by 0.06–0.09 (0.08–0.04) at $J = 10$–250 A/cm^2 compared with that of sample C (C_1), due to the reduction of well layer thickness. For the novel structure, the DOP of sample A is further decreased compared with that of samples B, while the DOP of sample A_1 is close to that of sample C_1 at the larger current density. It can be attributed to the band adjustment caused by the combination of barrier height and well layer coupling. By employing the coupled

well layer, the IQE of sample A (A_1) is also increased to 20.5% (14.8%) at $J = 100$ A/cm^2. In addition, the efficiency droop effect can be expected to be suppressed by using the novel structure.

References

[1] Hirayama H, Fujikawa S and Kamata N 2015 *Electronics and Communications in Japan* **98** 1

[2] Wang J, Yan J, Guo Y, Zhang Y, Tian Y, Zhu S, Chen X, Sun L and Li J 2015 *Scientia Sinica Physica, Mechanica & Astronomica* **45** 067303

[3] Saifaddin B, Almogbel A, Iza M, Albadri A, Al Yamani A, Nakamura S, Zollner C, Foronda H, Wu F, S. Speck J and DenBaars S P 2018 *Proc. SPIE* **10554** 1

[4] Nagasawa Y and Hirano A 2018 *Appl. Sci.* **8** 1264

[5] Li Y, Zhu Y, Wang M, Deng H and Yin H 2019 *Chin. Phys. B* **28** 097801

[6] Wang Y, Rong X, Ivanov S, Jmerik V, Chen Z, Wang H, Wang T, Wang P, Jin P, Chen Y, Kozlovsky V, Sviridov D E, Zverev M, Zhdanova E, Gamov N, Studenov V, Miyake H, Li H, Guo S, Yang X, Xu F, Yu T, Qin Z, Ge W, Shen B and Wang X 2019 *Adv. Opt. Mater.* **7** 1801763

[7] Takano T, Mino T, Sakai J, Noguchi N, Tsubaki K and Hirayama H 2017 *Appl. Phys. Express* **10** 031002

[8] Zhang Y, Zheng Y, Meng R, Sun C, Tian K, Geng C, Zhang Z H, Liu G and Bi W 2018 *IEEE Photon. J.* **10** 8200809

[9] Hideki H, Yusuke T, Tetsutoshi M and Norihiko K 2010 *Appl. Phys. Express* **3** 031002

[10] Li Y, Zhu Y, Wang M, Deng H and Yin H 2019 *Jpn. J. Appl. Phys.* **58** 114001

[11] Liu C, Ooi Y K, Islam S, Grace Xing H, Jena D and Zhang J 2018 *Appl. Phys. Lett.* **112** 011101

[12] Lu L, Wan Z, Xu F, Wang X, Lv C, Shen B, Jiang M and Chen Q 2017 *Superlattice Microst.* **104** 240

[13] Li Y, Zhu Y and Wang M 2019 *Journal of Nantong University (Natural Science Edition)* **18** 11 (in Chinese)

[14] Sato K, Yasue S, Ogino Y, Tanaka S, Iwaya M, Takeuchi T, Kamiyama S and Akasaki I 2019 *Appl. Phys. Lett.* **114** 191103

[15] Li Y, Zhu Y, Mei G, Wang M, Deng H and Yin H 2020 *Jpn. J. Appl. Phys.* **59** 084001

[16] Chuang S L and Chang C S 1996 *Phys. Rev. B* **54** 2491

[17] Chuang S L and Chang C S 1997 *Semicond. Sci. Tech.* **12** 252

[18] Wenzel H 2006 *Opt. Quantum Electron.* **38** 953

[19] Li Y, Zhu Y, Huang J, Deng H, Wang M and Yin H 2017 *J. Appl. Phys.* **121** 053105

[20] Kuo Y K, Chang J Y, Chang H T, Chen F M, Shih Y H and Liou B T 2017 *IEEE J. Quantum Electon.* **53** 1

[21] Long H, Wang S, Dai J, Wu F, Chen J, Liang R, Feng Z and Chen C 2018 *Opt Express* **26** 680

[22] Ni R, Yu Z, Liu Z, Zhang L, Jia L and Zhang Y 2020 *IEEE Photon. Technol. Lett.* **32** 971

[23] Yun J, Shim JI and Hirayama H 2015 *Appl. Phys. Express* **8** 022104